

## 结构锡靶激光等离子体极紫外光辐射特性研究

李镇广<sup>\*</sup>, 窦银萍<sup>\*</sup>, 谢卓, 王海建, 宋晓伟<sup>\*\*</sup>, 林景全

长春理工大学理学院, 吉林 长春 130022

**摘要** 开展结构 Sn 靶激光等离子体极紫外光辐射特性研究,对波长为 1064 nm 的脉冲激光等离子体产生的极紫外光谱进行研究。实验结果表明,当激光能量为 500 mJ,结构靶凹槽深度为 100  $\mu\text{m}$ 、宽度为 300  $\mu\text{m}$  时,结构靶凹槽产生 13.5 nm(2%带宽)带内光辐射积分强度的增强倍率约为平面靶的 1.57 倍。同时发现,凹槽对激光等离子体膨胀具有抑制作用,导致不同凹槽宽度产生最佳增强倍率所对应的激光能量不同。研究聚焦光斑尺寸对结构靶产生极紫外光辐射的影响。实验结果表明,当聚焦光斑直径与凹槽宽度接近时,凹槽的 13.5 nm(2%带宽)带内光辐射积分强度的增强倍率最高。此项研究对提高极紫外光辐射强度及转换效率具有重要意义。

**关键词** 光谱学; 极紫外辐射; 激光等离子体; 结构靶; 光刻光源

中图分类号 O434.13

文献标志码 A

doi: 10.3788/CJL202148.1601005

### 1 引言

激光等离子体极紫外光源在显微成像、材料分析以及极紫外光刻技术<sup>[1]</sup>等领域有着至关重要的作用。尤其极紫外光刻技术是制作 7 nm 以下节点集成电路所需的关键技术<sup>[2]</sup>,也是我国在高端芯片研发方面的短板。在极紫外光刻技术中,极紫外光源工作时需要使用与其配套的光学元件。对此,研究人员研制出的 Mo/Si 多层膜反射镜在 13.5 nm(2%带宽)内的反射率接近 70%<sup>[3]</sup>。因此,波长为 13.5 nm 的极紫外光源成为实现更小节点尺寸芯片所需的光刻光源<sup>[4]</sup>。近年来,研究人员开始对锂(Li)靶<sup>[5]</sup>、铑(Rh)靶<sup>[6]</sup>、氙(Xe)靶<sup>[7]</sup>和锡(Sn)靶<sup>[8]</sup>激光等离子体产生的 13.5 nm(2%带宽)带内极紫外光辐射特性以及转换效率进行了大量的研究。相比于其他的靶材,Sn 靶等离子体产生的极紫外光源具有较高的转换效率<sup>[8-9]</sup>,其在 13.5 nm(2%带宽)带内可产生高洁净度、宽带的光谱。此外,在产生光源的环境中充入稀有气体,可有效地减小光源离子碎屑的动能,延长光刻系统中光学元件的使用寿命<sup>[10]</sup>。以上特性使 Sn 靶 13.5 nm 极紫外光源成为极紫外光刻系统中需要的光源,对 Sn 靶 13.5 nm

光源的辐射特性进行研究具有一定的研究价值,使其在计量学以及极紫外光刻掩模检测等领域也有着重要的应用。

为了获得较高的转换效率来满足光刻系统所需的要求,研究人员通过改变激光波长<sup>[11]</sup>、脉冲宽度<sup>[12]</sup>、靶材密度<sup>[13]</sup>,利用双脉冲<sup>[14]</sup>等技术实现了较高的转换效率。此外,研究人员发现结构靶影响着极紫外光辐射强度以及转换效率。2004 年,Tanaka 等<sup>[15]</sup>利用 CO<sub>2</sub> 激光辐照纳米结构 Sn 靶,在 13.5 nm 处产生较强的极紫外光辐射,并且其光谱宽度窄于平面靶。2007 年,Ueno 等<sup>[16]</sup>利用深度为 200  $\mu\text{m}$  的 Sn 结构靶,获得极紫外光辐射的转换效率为 4%,这高于平面靶 2%的转换效率。2010 年,Harilal 等<sup>[1]</sup>使用凹槽 Sn 靶,通过凹槽壁对等离子体的膨胀进行有效约束,从而提高极紫外光辐射的转换效率,实验中获得极紫外光转换效率高达 5%。2014 年,Cummins 等<sup>[17]</sup>利用双脉冲辐照 Sn 楔形靶,得到 13.5 nm 处极紫外光辐射的转换效率为 3.6%。以上研究表明结构靶可以有效地提高极紫外光辐射的转换效率。然而,研究人员对于凹槽结构 Sn 靶的具体结构尺寸(包括凹槽宽度和凹槽深度)及其对极紫外光辐射的影响尚未进行系统

收稿日期: 2021-01-13; 修回日期: 2021-02-03; 录用日期: 2021-02-25

基金项目: 国家自然科学基金青年科学基金(62005021)、吉林省科技发展计划重点研发项目(20200401052GX)

通信作者: \*douzi714@126.com; \*\*songxiaowei@cust.edu.cn

研究。

本文系统地开展了凹槽结构靶对极紫外光辐射特性影响的研究。首先,固定凹槽宽度,研究了不同凹槽深度情况下产生的 13.5 nm(2%带宽)带内极紫外光辐射增强倍率与激光能量之间的依赖关系。其次,固定凹槽深度,研究了不同凹槽宽度情况下所产生的 13.5 nm(2%带宽)带内极紫外光辐射增强倍率与激光能量之间的依赖关系,获得产生最佳极紫外光辐射所对应的凹槽深度和宽度。最后,通过研究聚焦光斑尺寸对结构靶 13.5 nm(2%带宽)带内极紫外光辐射的影响,可为提高 13.5 nm(2%带宽)带内极紫外光辐射强度以及转换效率提供实验基础。实际极紫外光刻应用中采用激光辐照液滴锡靶来产生极紫外光源。但是由于液滴锡靶的实验难度和复杂性较高,为了减小实验难度,可利用固体结构靶来研究靶的特性对极紫外光源转换效率的影响。本文研究利用结构靶对等离子体的空间约束来提高 13.5 nm 极紫外光的转换效率。目前尚未有液滴锡靶中空间约束对等离子体极紫外辐射影响方面的研究报道。因此,该项工作的开展对通过进一步优化液滴靶来获得更高的极紫外光转换效率方面的研究有所帮助。

## 2 实验装置

激光辐照结构 Sn 靶等离子体极紫外光源的实验装置如图 1 所示。实验采用重复频率为 10 Hz、脉宽为 10 ns、输出波长为 1064 nm、最大能量为 800 mJ(Continuum, Powerlite Precision II)的激光器作为极紫外光辐射所需的激光光源。激光光束经过焦距为 400 mm 的透镜聚焦在尺寸为 400 mm×400 mm×5 mm 的靶材上面。为了方便对比平面

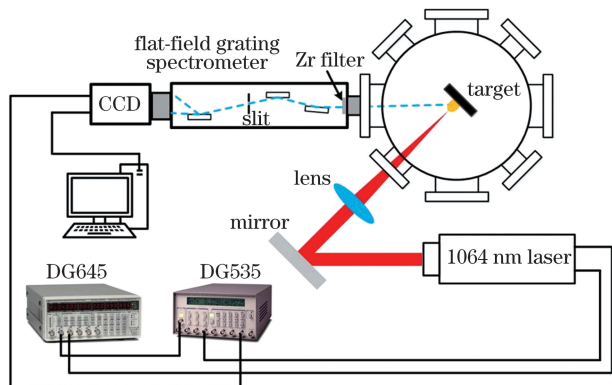


图 1 激光辐照结构靶等离子体极紫外光源实验装置

Fig. 1 Experimental setup of laser-produced plasma extreme ultraviolet light source using structured target

靶和结构靶所获得的实验结果,将同一块靶材分成平面靶和结构靶,并将靶材固定在三维平移台(Zolix SC300)上面,以保证每发激光都能够作用于全新的靶材。另外,通过移动聚焦透镜与靶材的相对距离,改变辐照在靶材表面的聚焦光斑大小。聚焦光斑大小的测量方法是:使用单发脉冲激光聚焦在平面靶材上面,利用金相显微镜获得不同条件下的烧蚀区域直径。

利用激光烧蚀方法制备不同凹槽尺寸的结构靶,通过控制烧蚀的范围,获得凹槽宽度为 100, 200, 300, 400  $\mu\text{m}$ 。同时,通过控制激光烧蚀的次数,获得不同的凹槽深度为 50, 100, 150, 200  $\mu\text{m}$ 。

激光等离子体产生的极紫外光辐射以与靶材法线方向呈  $45^\circ$  角入射至平像场光栅光谱仪中。光源先后经过厚度为 200 nm 的金属 Zr 膜、球面镜、柱面镜以及狭缝,最后以入射角为  $87^\circ$  入射至刻线为 1200 line/mm 的平场光栅表面,衍射的极紫外光被 X-ray CCD (Charge Couple Device) 所收集, CCD 曝光时间为 10 ms。采用数字延时发生器(Stanford Research, DG645 和 DG535)来控制激光脉冲与 CCD 之间的相对延时。整个实验过程中均采用单发模式,真空度约为  $10^{-3}$  Pa。

## 3 实验结果分析

首先,研究结构靶凹槽深度对极紫外光辐射的影响。实验中,固定入射激光能量为 500 mJ 和结构靶凹槽宽度为 300  $\mu\text{m}$ ,采用 0  $\mu\text{m}$ (固体平面靶)、50  $\mu\text{m}$ 、100  $\mu\text{m}$ 、150  $\mu\text{m}$ 、200  $\mu\text{m}$  的凹槽深度来对 13.5 nm(2%带宽)带内极紫外光辐射强度进行研究,实验结果如图 2 所示。图 2(a)所示为不同凹槽深度下所产生的极紫外光谱图,实验发现光谱在波长为 13.5 nm 附近产生了强烈的输出,其主要是由于  $\text{Sn}^{9+}$ - $\text{Sn}^{13+}$  离子在  $4p^6 4d^n - 4p^5 4d^{n+1} + 4p^6 4d^{n-1} 4f^{[18]}$  跃迁过程中产生不可分辨的跃迁阵列(UTA)而形成的宽带光谱<sup>[19]</sup>。此外,平面靶和结构靶产生的极紫外光谱轮廓相似,但是强度略有不同。对不同凹槽深度条件下 13.5 nm(2%带宽)带内极紫外光辐射强度进行积分并对其进行归纳总结,如图 2(b)所示。可以看出,结构靶条件下所产生的光谱强度均大于平面靶的情况,其主要原因是:激光入射至结构靶凹槽内时,与靶材相互作用产生激光等离子体并发生膨胀,此时凹槽壁对等离子体膨胀有抑制作用<sup>[1]</sup>,减小等离子体向外膨胀的速度,使等离子体保持一定的电子温度和电子密度,导致

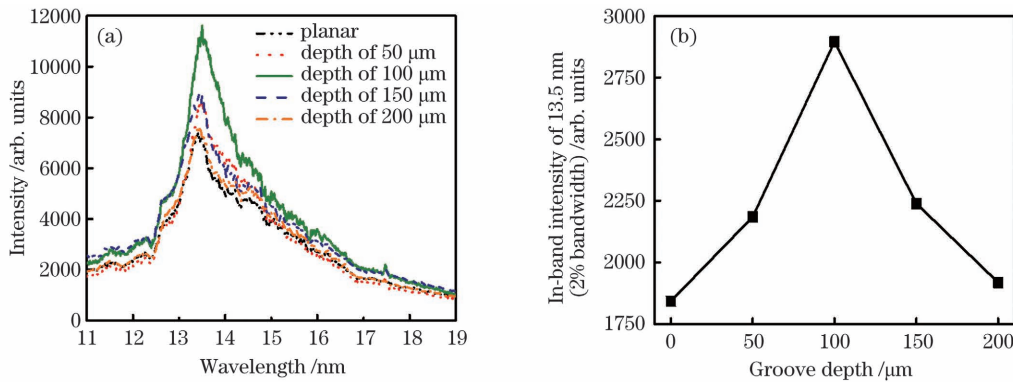


图 2 入射激光能量为 500 mJ、凹槽宽度为 300  $\mu\text{m}$ 、凹槽深度分别为 0, 50, 100, 150, 200  $\mu\text{m}$  情况下的极紫外光谱辐射图和 13.5 nm(2%带宽)带内光谱辐射的积分强度。(a)极紫外光谱辐射图;(b)13.5 nm(2%带宽)带内光谱辐射的积分强度随凹槽深度的变化

Fig. 2 Extreme ultraviolet radiation spectra and integral intensity of in-band radiation at 13.5 nm (2% bandwidth) when incident laser energy is 500 mJ, width of groove is 300  $\mu\text{m}$ , and groove depths are 0, 50, 100, 150, and 200  $\mu\text{m}$ . (a) Extreme ultraviolet radiation spectra; (b) integral intensity of in-band radiation at 13.5 nm (2% bandwidth) varying with groove depth

结构靶情况下所产生的 13.5 nm(2%带宽)带内极紫外光谱辐射强度较大。此外,13.5 nm(2%带宽)带内极紫外光谱积分强度随着凹槽深度的增加呈现先增大后减小的趋势,在凹槽深度为 100  $\mu\text{m}$  时产生的极紫外光谱辐射积分强度最强。造成这一现象的原因是,凹槽深度从 0~100  $\mu\text{m}$  增加的过程中,凹槽壁对激光等离子体膨胀的抑制作用逐渐增强,极紫外光谱强度亦逐渐增大;当凹槽深度大于 100  $\mu\text{m}$  时,受凹槽深度过大的影响,产生的部分极紫外光谱辐射未能从凹槽内辐射出来,进而导致光谱辐射减弱。由此得出只有凹槽深度为 100  $\mu\text{m}$  时光谱辐射积分强度最佳。

进一步地,固定结构靶凹槽宽度为 300  $\mu\text{m}$ ,在凹槽深度分别为 0  $\mu\text{m}$ 、50  $\mu\text{m}$ 、100  $\mu\text{m}$ 、150  $\mu\text{m}$  和 200  $\mu\text{m}$  情况下,对不同激光能量下所产生的极紫外光谱辐射特性进行研究。为了清晰看出凹槽深度对 13.5 nm(2%带宽)带内极紫外光谱辐射积分强度的影响,通过计算结构靶和平面靶两种情况下的 13.5 nm(2%带宽)带内光谱辐射积分强度的比值,获得不同凹槽深度下光谱辐射增强倍率与激光能量的关系,如图 3 所示。从图中可见,在不同激光能量下,凹槽深度为 100  $\mu\text{m}$  的结构靶激光等离子体产生的光谱辐射增强倍率始终高于凹槽深度为 50  $\mu\text{m}$ 、150  $\mu\text{m}$  和 200  $\mu\text{m}$  的情况。因此可知,改变激光能量对最佳凹槽深度的选择并没有影响。此外,随着激光能量从 100 mJ 增加到 800 mJ,4 种凹槽深度对应的增强倍率均呈现先增加后减小的趋势。当激光能量为 500 mJ 时,4 种凹槽深度对应的增强倍率均

达到最大值。此现象说明了激光能量依赖于凹槽宽度,也就是说不同凹槽宽度有可能对应着不同的最佳激光能量。为了验证上述观点,进行了凹槽宽度对极紫外光谱辐射强度的影响研究。

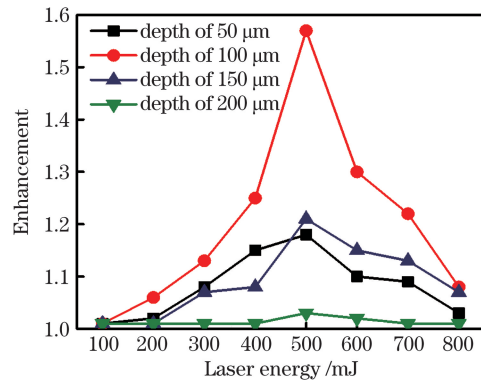


图 3 凹槽深度分别为 50, 100, 150, 200  $\mu\text{m}$  的 13.5 nm (2%带宽)带内光谱辐射的积分强度增强倍率与激光能量之间的关系,凹槽宽度为 300  $\mu\text{m}$

Fig. 3 Dependence of enhancement of 13.5 nm (2% bandwidth) in-band radiation intensity on incident laser energy under different groove depth (50, 100, 150, and 200  $\mu\text{m}$ ) and fixed groove width of 300  $\mu\text{m}$

首先固定激光能量和凹槽深度,研究结构靶凹槽宽度对极紫外光谱辐射特性的影响。实验过程中,固定激光能量为 500 mJ 和凹槽深度为 100  $\mu\text{m}$ ,采用凹槽宽度分别为 100  $\mu\text{m}$ 、200  $\mu\text{m}$ 、300  $\mu\text{m}$ 、400  $\mu\text{m}$  的结构靶来研究 13.5 nm(2%带宽)带内极紫外光源辐射强度的变化规律,实验结果如图 4 所示。从图 4(a)中可以看出,不同凹槽宽度下产生的 13.5 nm 极紫外光谱辐射强度也均大于平面靶的情

形。结合图 2 可进一步说明,结构靶可以有效地增加极紫外光谱辐射强度。对不同凹槽宽度下 13.5 nm(2%带宽)带内极紫外光谱辐射强度进行积分并对其进行归纳总结,结果如图 4(b)所示。随着凹槽宽度的增加,13.5 nm(2%带宽)带内光谱辐射积分强度呈现先增大后减小的趋势,在凹槽宽度为 300  $\mu\text{m}$  处光谱辐射积分强度达到最强。产生这种现象的原因是:当凹槽宽度较小(小于激光聚焦光

斑)时,部分激光脉冲能量无法辐照到凹槽内进行有效的耦合,导致光谱辐射强度增强不明显;当凹槽宽度较大时,凹槽壁不能有效抑制等离子体膨胀,同样导致光谱辐射强度增强较慢。只有当注入凹槽的激光能量与等离子体膨胀相互平衡时,产生的极紫外光谱辐射最强。本实验中,最大 13.5 nm(2%带宽)带内极紫外光谱辐射积分强度所对应的凹槽宽度为 300  $\mu\text{m}$ 。

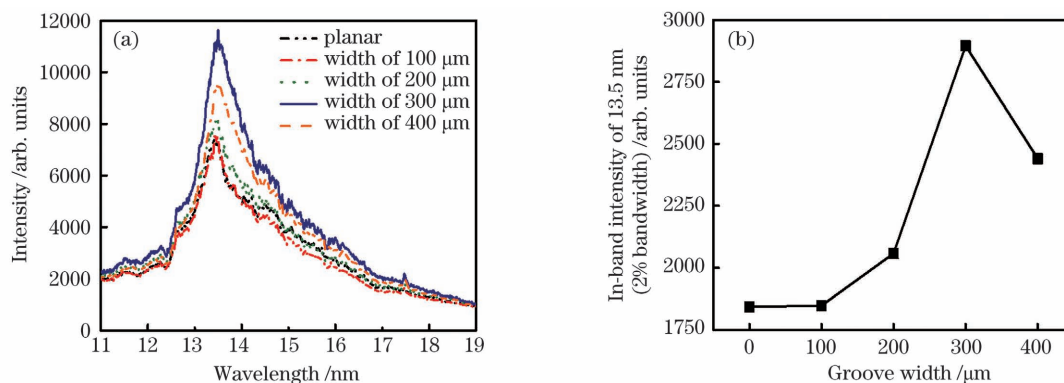


图 4 入射激光能量为 500 mJ、凹槽深度为 100  $\mu\text{m}$ 、凹槽宽度分别为 100, 200, 300 and 400  $\mu\text{m}$  情况下的极紫外光谱辐射图和 13.5 nm(2%带宽)带内光谱辐射的积分强度。(a)极紫外光谱辐射图;(b)13.5 nm(2%带宽)带内光谱辐射的积分强度随凹槽宽度的变化

Fig. 4 Extreme ultraviolet radiation spectra and integral intensity of in-band radiation at 13.5 nm (2% bandwidth) when incident laser energy is 500 mJ, depth of groove target is 100  $\mu\text{m}$ , and groove widths are 100, 200, 300, and 400  $\mu\text{m}$ . (a) Extreme ultraviolet radiation spectra; (b) integral intensity of in-band radiation at 13.5 nm (2% bandwidth) varying with groove width

接下来,固定凹槽深度为 100  $\mu\text{m}$ ,研究不同凹槽宽度下结构靶所产生的 13.5 nm(2%带宽)带内光谱辐射积分强度的增强倍率随入射激光能量的变化趋势,结果如图 5 所示。随着入射激光能量从 100 mJ 增加至 800 mJ,4 种凹槽宽度对应的增强倍率均呈先增加后减小的趋势,但是增强倍率达到最大值时的入射激光能量不同。此现象很好地说明了实现最大增强倍率所需的最佳激光能量与凹槽宽度有关,结构靶凹槽宽度越大,对应的激光能量越大。其原因在于激光能量逐渐增加时,等离子体的热能也在增加,进而导致激光等离子体的纵向(垂直于激光入射方向)膨胀区域变大。因此,在改变激光能量时,需要与其相对应的凹槽宽度来对等离子体膨胀进行有效抑制以获得更强的极紫外光谱辐射,即小激光能量对应窄的凹槽,大激光能量对应宽的凹槽。本实验中,在凹槽深度为 100  $\mu\text{m}$ 、宽度为 300  $\mu\text{m}$  以及激光能量为 500 mJ 时,得到 13.5 nm(2%带宽)带内极紫外光谱辐射积分强度的增强倍率为 1.57。由此可见,结构靶在提高极紫外光谱辐射强度方面具有一定的潜力。

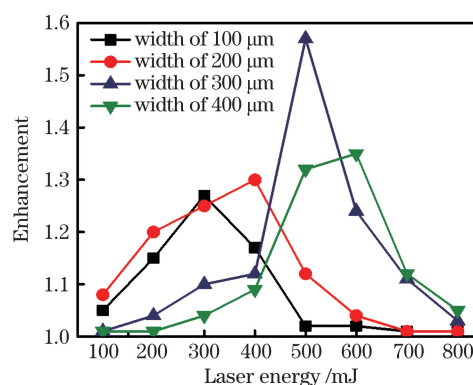


图 5 凹槽宽度分别为 100, 200, 300, 400  $\mu\text{m}$  的 13.5 nm(2%带宽)带内光谱辐射的积分强度增强倍率与激光能量之间的关系,凹槽深度为 100  $\mu\text{m}$

Fig. 5 Dependence of enhancement of 13.5 nm (2% bandwidth) in-band radiation intensity on incident laser energy under different groove width (100, 200, 300, and 400  $\mu\text{m}$ ) and fixed groove depth of 100  $\mu\text{m}$

最后,固定激光能量为 500 mJ,结构靶凹槽深度为 100  $\mu\text{m}$ 、宽度为 300  $\mu\text{m}$  时,研究聚焦光斑尺寸对 13.5 nm(2%带宽)带内极紫外光谱辐射强度的影

响。不同聚焦光斑尺寸下的结构靶与平面靶所产生的 13.5 nm(2%带宽)带内光辐射积分强度的增强倍率如图 6 所示。随着光斑尺寸的增加,增强倍率呈现先增加后减小的趋势,光斑直径约为 290  $\mu\text{m}$  时增强倍率最大。然而,在聚焦光斑尺寸较小时,增强倍率最小。此现象说明了聚焦光斑较小时,大部分激光能量用来加快等离子体纵向膨胀,只有少部分能量用来产生极紫外光辐射<sup>[20]</sup>,导致两种靶材所产生的极紫外光辐射强度比较相近。随着光斑尺寸的进一步增加,等离子体的纵向膨胀减少,大部分能量用来转化 13.5 nm(2%带宽)带内极紫外光辐射。此外,对于凹槽靶来说,聚焦光斑直径与凹槽宽度值相近时,其能够与凹槽进行有效的耦合,进而产生较强的 13.5 nm(2%带宽)带内光辐射。Harilal 等<sup>[1]</sup>的研究结果表明,当聚焦光斑直径为结构靶凹槽宽度的 1 倍左右时,所产生的极紫外光转换效率最高。所得实验结果也很好证实了上述结论。

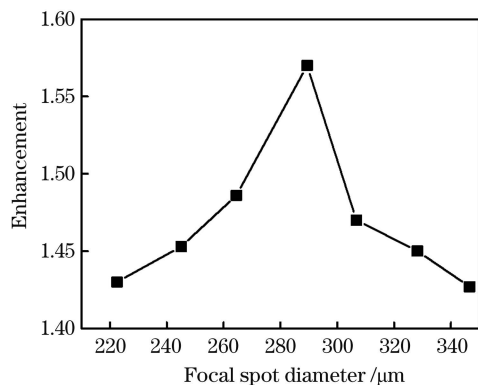


图 6 激光能量为 500 mJ,结构靶凹槽深度为 100  $\mu\text{m}$ 、宽度为 300  $\mu\text{m}$  时,激光聚焦光斑直径对结构靶产生的 13.5 nm(2%带宽)带内光谱辐射的积分强度增强倍率的影响

Fig. 6 Dependence of enhancement of 13.5 nm(2% bandwidth) in-band radiation integral intensity on focal spot diameter when incident laser energy is 500 mJ, groove depth is 100  $\mu\text{m}$ , and groove width is 300  $\mu\text{m}$

## 4 结 论

开展了结构 Sn 靶激光等离子体极紫外光辐射研究。实验结果表明,固定凹槽宽度为 300  $\mu\text{m}$  时,在不同凹槽深度下,产生最佳 13.5 nm(2%带宽)光辐射积分强度所对应的激光能量均为 500 mJ。同时,凹槽深度较大会减弱极紫外光从凹槽内向外辐射的强度,在凹槽深度为 100  $\mu\text{m}$  时,13.5 nm(2%带宽)光辐射积分强度最佳。此外,固定凹槽深度为

100  $\mu\text{m}$  时,在不同凹槽宽度下,产生最佳 13.5 nm(2%带宽)光辐射积分强度所对应的激光能量不同。随着凹槽宽度的增加,对应的最佳激光能量也在增加。此现象很好地说明了结构靶凹槽壁对激光等离子体膨胀有抑制作用,能够增强极紫外光辐射强度。聚焦光斑尺寸对结构靶 13.5 nm(2%带宽)光辐射影响的实验结果表明,聚焦光斑直径约为 300  $\mu\text{m}$  且与凹槽宽度相接近时,产生的 13.5 nm(2%带宽)光辐射最佳。综上,当激光能量为 500 mJ,凹槽深度为 100  $\mu\text{m}$ 、宽度为 300  $\mu\text{m}$  时,产生的 13.5 nm(2%带宽)极紫外光辐射积分强度增强倍率为平面靶情形的 1.57 倍,说明 13.5 nm(2%带宽)极紫外光辐射的输出能量得到提高。

## 参 考 文 献

- [1] Harilal S S, Sizyuk T, Sizyuk V, et al. Efficient laser-produced plasma extreme ultraviolet sources using grooved Sn targets [J]. *Applied Physics Letters*, 2010, 96(11): 111503.
- [2] Xie W L, Wu X B, Wang K B, et al. Effect of EUV source parameters on focused beam performance of EUV radiation-damage-test system [J]. *Chinese Journal of Lasers*, 2020, 47(6): 0601004.  
谢婉露, 吴晓斌, 王魁波, 等. 极紫外光源参数对极紫外辐照损伤测试系统聚焦光束性能的影响[J]. *中国激光*, 2020, 47(6): 0601004.
- [3] Freitag J M, Clemens B M. Stress evolution in Mo/Si multilayers for high-reflectivity extreme ultraviolet mirrors[J]. *Applied Physics Letters*, 1998, 73(1): 43-45.
- [4] Zhao Y P, Xu Q, Li Q, et al. 13.5 nm extreme ultraviolet light source based on discharge produced Xe plasma[J]. *Chinese Journal of Lasers*, 2018, 45(11): 1100001.  
赵永蓬, 徐强, 李琦, 等. 13.5 nm 放电 Xe 等离子体极紫外光源[J]. *中国激光*, 2018, 45(11): 1100001.
- [5] Schriever G, Mager S, Naweed A, et al. Laser-produced lithium plasma as a narrow-band extended ultraviolet radiation source for photoelectron spectroscopy[J]. *Applied Optics*, 1998, 37(7): 1243-1248.
- [6] Nagano A, Inoue T, Nica P E, et al. Extreme ultraviolet source using a forced recombination process in lithium plasma generated by a pulsed laser [J]. *Applied Physics Letters*, 2007, 90(15): 151502.
- [7] Ueno Y, Ariga T, Soumagne G, et al. Efficient extreme ultraviolet plasma source generated by a CO<sub>2</sub> laser and a liquid xenon microjet target[J]. *Applied*

- Physics Letters, 2007, 90(19): 191503.
- [8] Harilal S S, Tillack M S, Tao Y, et al. Extreme-ultraviolet spectral purity and magnetic ion debris mitigation by use of low-density tin targets [J]. Optics Letters, 2006, 31(10): 1549-1551.
- [9] Tao Y, Tillack M S, Harilal S S, et al. Investigation of the interaction of a laser pulse with a preformed Gaussian Sn plume for an extreme ultraviolet lithography source [J]. Journal of Applied Physics, 2007, 101(2): 023305.
- [10] Bollanti S, Bonfigli F, Burattini E, et al. High-efficiency clean EUV plasma source at 10–30 nm, driven by a long-pulse-width excimer laser [J]. Applied Physics B, 2003, 76(3): 277-284.
- [11] Koshelov K, Krivtsun V, Gayasov R, et al. Experimental study of laser produced gadolinium plasma emitting at 6.7 nm [R]. Dublin: International Workshop on EUV source, 2010: P31.
- [12] Ando T, Fujioka S, Nishimura H, et al. Optimum laser pulse duration for efficient extreme ultraviolet light generation from laser-produced tin plasmas [J]. Applied Physics Letters, 2006, 89(15): 151501.
- [13] Otsuka T, Kilbane D, Higashiguchi T, et al. Systematic investigation of self-absorption and conversion efficiency of 6.7 nm extreme ultraviolet sources [J]. Applied Physics Letters, 2010, 97(23): 231503.
- [14] Lin J Q, Tomie T. Enhancement of EUV emission intensity from particles in a droplet by exploding the droplet [J]. Journal of Physics D: Applied Physics, 2009, 42(15): 155203.
- [15] Tanaka H, Akinaga K, Takahashi A, et al. Development of a target for laser-produced plasma EUV light source using Sn nano-particles [J]. Applied Physics A, 2004, 79(4/5/6): 1493-1495.
- [16] Ueno Y, Soumagne G, Sumitani A, et al. Enhancement of extreme ultraviolet emission from a CO<sub>2</sub> laser-produced Sn plasma using a cavity target [J]. Applied Physics Letters, 2007, 91 (23): 231501.
- [17] Cummins T, O’Gorman C, Dunne P, et al. Colliding laser-produced plasmas as targets for laser-generated extreme ultraviolet sources [J]. Applied Physics Letters, 2014, 105(4): 044101.
- [18] Churilov S S, Ryabtsev A N. Analyses of the Sn IX–Sn XII spectra in the EUV region [J]. Physica Scripta, 2006, 73(6): 614-619.
- [19] White J, Dunne P, Hayden P, et al. Optimizing 13.5 nm laser-produced tin plasma emission as a function of laser wavelength [J]. Applied Physics Letters, 2007, 90(18): 181502.
- [20] Harilal S S, Coons R W, Hough P, et al. Influence of spot size on extreme ultraviolet efficiency of laser-produced Sn plasmas [J]. Applied Physics Letters, 2009, 95(22): 221501.

## Characteristics of Extreme Ultraviolet Emission from Laser-Produced Plasma on Structured Sn Target

Li Zhenguang, Dou Yinpíng<sup>\*</sup>, Xie Zhuo, Wang Haijian, Song Xiaowei<sup>\*\*</sup>, Lin Jingquan

*School of Science, Changchun University of Science and Technology, Changchun, Jilin 130022, China*

### Abstract

**Objective** Extreme ultraviolet (EUV) radiation plays significant roles in various field applications, such as microscopy imaging, material analysis, and EUV lithography. In particular, EUV lithography is an important technology for manufacturing integrated circuits with a feature size less than 7 nm. Compared with the fuel materials of Li and Xe for EUV radiation, the tin (Sn) plasma EUV radiation has purity, broadband spectra, and high conversion efficiency at 13.5 nm. In addition, the EUV radiation with 2% bandwidth centered at 13.5 nm wavelength can be reflected by Mo and Si multilayer optical devices. The above features make the 13.5 nm EUV radiation of Sn become the source of the EUV lithography system. In practical EUV lithography applications, the Sn droplet target is selected as the source for lithography. However, the difficulties in experiment and complexity are expected when Sn droplet EUV radiation is generated. For simply studying the conversion efficiency of Sn droplet EUV radiation, we can use the metal target to replace the droplet target. In this study, we report the 13.5 nm EUV radiation from laser-produced plasma on the structured target can optimize the conversion efficiency. To the best of our knowledge, no studies have been reported on the effect of spatial constraints on EUV radiation in Sn droplet targets. This work may be helpful for further research on optimizing droplet targets to obtain higher EUV conversion

efficiency.

**Methods** The EUV spectra from plasma are created by an 800 mJ, 10 ns full width at half maximum, and 1064 nm Nd : YAG laser pulse. The groove structured Sn target is fabricated by laser ablation. The width and depth of various grooves are obtained by adjusting the ablation area and times, respectively. The target is controlled by a translating stage to ensure that each laser pulse can radiate in a fresh position. The laser is focused onto the structured target by a plano-concave lens with a focal length of 400 mm. The laser focal spot diameter is changed by moving the distance between the lens and the target surface. The EUV spectra are measured by a flat-field spectrometer with a charge-coupled device (CCD) camera, which is placed at 45° with respect to the direction of the incident laser beam. Two digital delay generators are employed to control the delay time between the laser pulse and the CCD camera.

**Results and Discussions** The EUV in-band radiation (2% bandwidth centered at 13.5 nm) from the structured targets is found to be stronger than that from the planar targets. Results show that the enhanced EUV radiation can be obtained due to the plasma expansion restricted by the grooved wall. First, when fixing the groove width, the intensity of in-band radiation at 13.5 nm (2% bandwidth) increases and then drops with increasing groove depth from 50  $\mu\text{m}$  to 200  $\mu\text{m}$ . The optimal groove depth for EUV emission around 13.5 nm is 100  $\mu\text{m}$ . However, when the depth of the groove is larger than 100  $\mu\text{m}$ , part of the EUV radiation is blocked by the wall of the groove. However, when the groove depth is less than 100  $\mu\text{m}$ , the confinement effect of the grooved wall is relatively small (Fig. 2). In addition, the laser energy that corresponds to the highest EUV in-band radiation enhancement is found to be 500 mJ for different groove depths when fixing the groove width at 300  $\mu\text{m}$ . It means that the optimal laser energy may be influenced by the groove width, rather than the groove depth (Fig. 3). Moreover, when fixing the groove depth of 100  $\mu\text{m}$  and the laser energy of 500 mJ, the highest EUV in-band radiation intensity is obtained with the optimal groove width of 300  $\mu\text{m}$  for different groove widths. This attributes that the groove width is larger than 300  $\mu\text{m}$ , and that the confinement effect from the grooved wall is reduced. When the groove width is less than 300  $\mu\text{m}$ , the part of the laser energy cannot be coupled into the groove and interact with the target (Fig. 4). When the groove depth is fixed at 100  $\mu\text{m}$ , the laser energies that correspond to the highest enhancement of the EUV in-band radiation are varied with different groove widths. Meanwhile, the optimal laser energy increases as the groove width increases. It means that the groove width is related to the laser energy (Fig. 5). However, when the focal spot diameter is close to the optimal groove width of 300  $\mu\text{m}$ , the highest in-band radiation enhancement is obtained.

**Conclusions** In this study, EUV radiation emitted by laser-produced plasma from a structured target is conducted. The results show that the laser energy that corresponds to the optimal in-band intensity of 13.5 nm (2% bandwidth) is 500 mJ, regardless of the groove depth when the groove width is fixed at 300  $\mu\text{m}$ . In addition, the in-band EUV radiation with the groove depth of 100  $\mu\text{m}$  is stronger than that in the other cases. Further, when the groove depth is fixed at 100  $\mu\text{m}$ , for different groove widths, the highest EUV in-band radiation intensity depends on the laser energy. Meanwhile, the optimal laser energy increases as groove width increases. This phenomenon illustrates that the groove wall can effectively restrict plasma expansion. This confinement effect can enhance the EUV radiation. However, the highest in-band EUV radiation is obtained when the focal spot diameter is close to the groove width of 300  $\mu\text{m}$ . In summary, a 1.57-fold enhancement of the in-band EUV emission is obtained using the structured Sn target with 100  $\mu\text{m}$  depth and 300  $\mu\text{m}$  width when the laser energy is 500 mJ. This study is of great significance to improve the EUV radiation intensity and conversion efficiency.

**Key words** spectroscopy; extreme ultraviolet radiation; laser-produced plasma; structured target; lithography light source

**OCIS codes** 300.6560; 340.7480; 350.5400